

H. YONG-JIE^{1,2}, L. YUN-MING^{1,2*}, H. CHENG-YONG^{1,3}, M.M. AL BAKRI ABDULLAH^{1,2},
O. SHEE-WEEN^{1,2}, T. HOE-WOON^{1,3}, L. JIA-NI^{1,2}, Y. YU-XIN^{1,2}, M. NABIAŁEK⁴

HEAT-TREATED FLY ASH-CALCIUM HYDROXIDE GEOPOLYMERS: ENHANCING MECHANICAL AND MORPHOLOGICAL PERFORMANCES

The combined effect of calcium hydroxide (CH) and heat treatment on mechanical and morphological performances of geopolymer remains underexplored, presenting a critical gap in heat-resistance geopolymer research. This paper investigates the effect of CH (0, 2, and 4 wt.%) and elevated temperatures (200-1000°C) on the mechanical and morphological properties of fly ash (FA) geopolymers. The addition of 2 wt.% of CH enhanced compressive strength (35.8 MPa), attributed to coexistence of N-A-S-H and C-S-H, which enhanced structural interlocking and reinforced the compactness. At 200°C, FA geopolymers developed a robust structure due to further geopolymerization; however, structural deterioration occurred at 800-1000°C due to the melting of geopolymer gels and further phase transformation. This study provided guidelines for synthesizing sustainable and thermally resistant construction binders, particularly for applications in industrial flooring and thermal insulation structural walls.

Keywords: Calcium hydroxide; elevated temperature; compressive strength; morphology

1. Introduction

In recent years, production of ordinary Portland cement (OPC) has drastically increased, contributing to 5%-8% of worldwide carbon dioxide (CO₂) emissions [1]. Geopolymers are eco-friendly cementitious binders that serve as an alternative to OPC. The geopolymers are synthesized by polymerizing aluminosilicate precursors with alkaline solutions. Specifically, the aluminosilicate precursors dissolve in the alkaline solutions, releasing silica (SiO₂) and alumina (Al₂O₃), which then reorganize and undergo polycondensation to form a stable geopolymer network. In comparison to OPC, geopolymers offer more outstanding performance, including strength development [2], thermal stability [3] and durability [4]. Besides, the production of geopolymers significantly reduces CO₂ emission by 26%-45% [5]. Fly ash (FA), which is an industrial waste material generated over 500 million tons annually from power plants [6], is particularly suitable for geopolymer formation due to its high SiO₂ and Al₂O₃ content [7].

Calcium (Ca) can act as a supplementary binder in geopolymer formation since it can partially replace the alkali

in the geopolymerization reaction [8]. This substitution favors the formation of Ca-based hydration products, refining the lattice structure and strengthening the geopolymer matrix. For instance, Janga et al. [9] reported that incorporating steel slag, with high Ca content, into FA geopolymers led to the formation of calcium-silicate-hydrate (C-S-H), enhancing mechanical integrity. However, steel slag, an industrial waste product, possessed a glassy structure with semi-crystalline phases, resulting in partially stable state that restricts its reactivity [10]. Therefore, calcium hydroxide (CH) is a highly promising source of Ca for geopolymer formation. The inclusion of CH accelerated the reaction kinetics of the metakaolin geopolymers, resulting in a strength increment of 6% [11]. Borcato et al. [12] synthesized a metakaolin geopolymers with the addition of CH that exhibited a compressive strength of approximately 50.0 MPa. Hence, CH proved advantageous for enhancing the performance of the geopolymers and was thus utilized in the present study.

When temperatures exceeded 400°C, OPC undergoes strength degradation. In contrast, heat-treated geopolymers exhibited a smoother texture and greater strength. Samadi et al. [13]

¹ UNIVERSITI MALAYSIA PERLIS (UNIMAP), CENTRE OF EXCELLENCE FOR GEOPOLYMER AND GREEN TECHNOLOGY (CEGEOGTECH), 02600 ARAU, PERLIS, MALAYSIA

² UNIVERSITI MALAYSIA PERLIS (UNIMAP), FACULTY OF CHEMICAL ENGINEERING AND TECHNOLOGY, 02600 PERLIS, MALAYSIA

³ UNIVERSITI MALAYSIA PERLIS (UNIMAP), FACULTY OF MECHANICAL ENGINEERING AND TECHNOLOGY, 02600 PERLIS, MALAYSIA

⁴ CZESTOCHOWA UNIVERSITY OF TECHNOLOGY, FACULTY OF PRODUCTION ENGINEERING AND MATERIALS TECHNOLOGY, DEPARTMENT OF PHYSICS, 19 ARMII KRAJOWEJ AV., 42-200 CZESTOCHOWA, POLAND

* Correspondence address: ymliew@unimap.edu.my



claimed that FA geopolymer concretes experienced a 31.8% strength increment as temperatures rose to 200°C. Moreover, Verma et al. [14] reported that FA geopolymers retained 60.0% of their compressive strength without structural deterioration even when exposure to 700°C. Geopolymers possessed better spalling resistance, attributed to their interconnected pore channels that allowed internal pressure to escape and prevented stress buildup within the matrix [15]. Apart from that, Alventosa et al. [16] fabricated metakaolin geopolymers with 10 wt.% of CH and reported that the addition of CH reduced porosity beyond 600°C due to extensive densification and phase transformation. Yet, the mechanism underlying this behavior remains unexplored, with limited studies examining the combined effect of CH incorporation and heat treatment on the mechanical and morphological properties of geopolymers. Notably, CH incorporation significantly alters the microstructure, thereby impacting mechanical performance, morphology, and thermal stability. A comprehensive investigation into the relationship between CH incorporation and heat treatment is crucial for enhancing the heat resistance of geopolymers and advancing their real-world applications.

This work is intended to develop sustainable, thermally resistant construction binders by incorporating CH in FA geopolymers. This study primarily investigated the effect of CH incorporation (0, 2, and 4 wt.%) and elevated temperatures (200, 400, 600, 800, and 1000°C) on the mechanical and morphological properties of FA geopolymers. The bulk density and compressive strength of untreated and heat-treated geopolymers were evaluated. To gain deeper insights, the morphology and functional groups of the untreated and heat-treated geopolymers were also examined. This study provided a comprehensive understanding of how CH changes the mechanical strength and microstructure of the geopolymers under elevated temperatures. Moreover, it offered valuable guidelines for synthesizing heat-resistance construction binders, particularly for industrial stakeholders.

2. Experimental

FA was sourced from Tenaga Nasional Berhad (TNB) Janamanjung power plant in Perak, Malaysia. The FA was received as a fine, dark grey color powder, with its chemical compositions detailed in TABLE 1. The FA was predominantly composed of SiO₂ (38.8%), Fe₂O₃ (19.5%), CaO (18.1%), and Al₂O₃ (14.7%), which were classified as Class F according to ASTM C618. The alkaline solution used was a combination of sodium silicate (Na₂SiO₃) and sodium hydroxide (NaOH). The Na₂SiO₃ was in liquid form, obtained from South Pacific Chemical Industries Sdn. Bhd., Malaysia. It had an alkali modulus (SiO₂/Na₂O) of 3.2 and consisted of 39.5% Na₂SiO₃ and 60.5% water (H₂O). Besides, the NaOH, provided by Formosa Plastic Corporation, Taiwan, was in the form of caustic soda flakes with a purity of 99%. The CH utilized in the present study was supplied by Sigma-Aldrich Corporation. It demonstrated a powdered form with a white appearance.

TABLE 1

Chemical composition of FA

Chemical compositions	Weight percentages (wt.%)
SiO ₂	38.8
Al ₂ O ₃	14.7
Fe ₂ O ₃	19.5
CaO	18.1
SO ₃	1.5
K ₂ O	1.8
Others	5.6

Initially, a 10 M of NaOH solution was prepared by dissolving NaOH pellets in distilled water and allowed to cool down before use. The Na₂SiO₃ solution was subsequently mixed with NaOH solution to prepare an alkaline solution. The mix proportions of CH-incorporated FA geopolymers are presented in TABLE 2. The FA was mixed with the alkaline solution until a uniform slurry was achieved. CH was incorporated into the slurry at weight percentages (wt.%) of 0, 2, and 4, and stirred continuously to produce a homogeneous geopolymer mixture. The geopolymer mixture was cast into molds with a dimension of 50×50×50 mm³ and compacted to remove the entrapped air bubbles. The geopolymers were cured at room temperature and demolded after 24 h. The geopolymers were then oven-cured at 60°C for another 24 h to ensure stability. After that, the geopolymers were sealed and stored at room temperature for 26 days prior to testing and analysis. The 28 days-aged geopolymers were heat-treated in a muffle furnace at 200, 400, 600, 800, and 1000°C, with a heating rate of 10°C/min and a soaking period of 2 h. A set of geopolymers with varied CH concentrations remained untreated for comparison purposes.

TABLE 2

Mix proportions of CH-incorporated FA geopolymers

Mix proportions	CH incorporated FA geopolymers
NaOH concentration	10 M
Solid-to-liquid (S/L) ratio	2.5
Na ₂ SiO ₃ -to-NaOH (SS/SH) ratio	2.5
CH content	0, 2, and 4 wt.%

The bulk density test was conducted by measuring the volume and weight of both untreated and heat-treated geopolymers, following ASTM C138. The compressive strength of the geopolymers was tested using Instron series 5569 with a loading rate of 5 mm/min, in accordance with ASTM C109. Three replicates were carried out to obtain the average compressive strength values for both untreated and heat-treated geopolymers. The microstructure of untreated and heat-treated geopolymers was examined utilizing a Scanning Electron Microscopy (SEM) modeled JEOL JSM-6460LA. The geopolymer pieces were placed on carbon tape and coated with platinum using an Auto Finer Coater. Perkin Elmer Fourier Transform Infrared (FTIR) RXI spectroscopy was used to analyze the functional groups of the untreated and heat-treated geopolymers in the range of 500-4000 cm⁻¹.

3. Results and discussions

Fig. 1 illustrates the physical appearance of FA geopolymers with varying CH content after heat treatment. A significant color change was observed, as the geopolymers initially exhibited shades of grey before heat exposure, ranging from dark grey (2 wt.%) to light grey (4 wt.%). The darker tone was attributed to the higher iron (Fe) content in FA, whereas the lighter shade resulted from the white-colored CH [17]. As the temperature rose, the color of the FA geopolymers changed to yellowish at 600°C, and then to brownish at 800 and 1000°C. These color changes were accounted for the oxidation of Fe components and phase transformation [18,19].

Moreover, the incorporation of CH substantially increased pore formation in the FA geopolymers. This was ascribed to the chemical reaction between CH, SiO₂ and Al₂O₃, which gener-

ated additional H₂O that became trapped within the structure and subsequently evaporated upon heat exposure, leading to greater porosity inside the matrix. As evidence, the geopolymers with 4 wt.% CH demonstrated significantly higher porosity, which was visibly apparent. Regardless of the CH content, heat treatment facilitated surface cracks in FA geopolymers, particularly at 800 and 1000°C. The FA geopolymers with 2 wt.% CH demonstrated minimal cracking (Fig. 1b), likely due to the optimal CH content promoting the compactness of the structure. However, at 1000°C, the number and width of cracks gradually increased with higher CH content (4 wt.%), indicating its detrimental effect on the physical integrity of the FA geopolymers.

Fig. 2 depicts the bulk density of FA geopolymers with the incorporation of CH before and after heat treatment. The bulk density of untreated FA geopolymer was 1.7 g/cm³ and increased to 1.8 g/cm³ as the CH content raised from 0 to 2 wt.%. This sug-

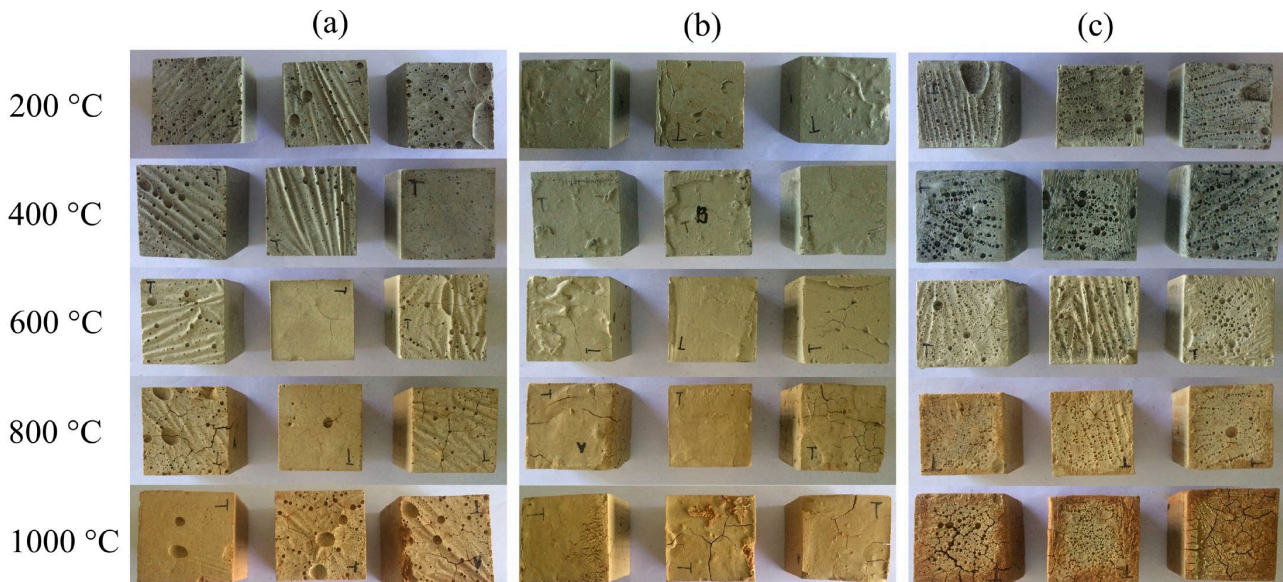


Fig. 1. Physical appearance of heat-treated FA geopolymers with (a) 0 wt.%, (b) 2 wt.%, and (c) 4 wt.% of CH contents

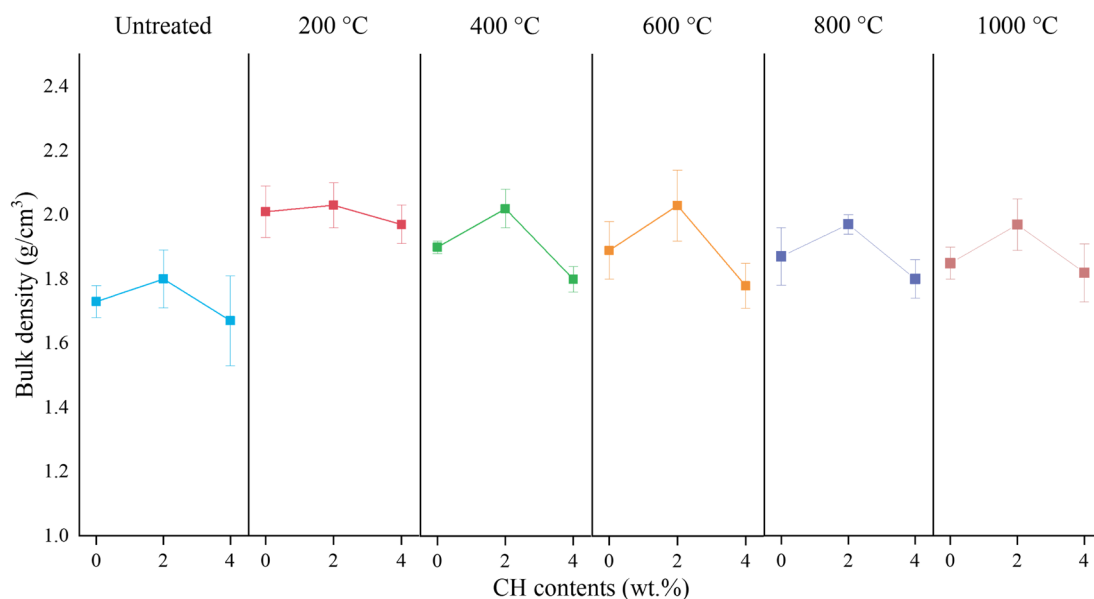


Fig. 2. Bulk density of untreated and heat-treated FA geopolymers with varying CH contents

gested that an incorporation of CH can effectively improve the bulk density of the FA geopolymers, as additional Ca enhanced the hydration reaction, resulting in a denser structure [20]. Ma et al. [11] reported that CH integration increased the density of metakaolin-based geopolymers. The greater amount of CH promoted the chemical reactions by converting free water into bound water, reducing porosity. However, in FA geopolymers, excessive CH content triggered rapid precipitation, hindering geopolymerization and limiting geopolymer network formation, significantly lowering density. As a result, with a further increase in CH to 4 wt.%, the bulk density of the FA geopolymers dropped to 1.7 g/cm³.

The bulk density of the CH-incorporated FA geopolymers shows an increasing trend when subjected to 200°C. As shown, those with CH content of 0, 2, and 4 wt.% displayed density gains of 16.2%, 12.8%, and 18.0%, respectively. This densification was related to the moisture loss and the continuous geopolymerization reaction. In contrast, the further increase in temperatures reduced the bulk density of the CH-incorporated FA geopolymers. Above 400°C, the bulk density of the FA geopolymers with and without the incorporation of CH significantly decreased, except for those with 2 wt.% CH. The decrement was attributed to the diminishment of physically bonded water and the phase transformation of the geopolymer structure.

Moreover, the FA geopolymer with 2 wt.% CH retained the highest bulk density after heat treatment. This was attributed to the presence of Ca²⁺ ions from CH, which polymerized with Si⁴⁺ from FA, facilitating C-S-H formation, as aforementioned. This C-S-H enhanced structural compactness by refining the pores inside the FA geopolymers [21]. Meanwhile, Si⁴⁺ and Al³⁺ from FA reacted with Na⁺ from the alkali activators (Na₂SiO₃ and NaOH), promoting the formation of sodium-aluminosilicate-hydrate (N-A-S-H), a typical gel phase in FA geopolymers [22]. The coexistence of N-A-S-H and C-S-H gels resulted in a highly densified geopolymer matrix, thereby reinforcing thermal stability of the CH-incorporated FA geopolymers.

The compressive strength of FA geopolymers, both with and without the incorporation of CH, after being subjected to heat treatment is shown in Fig. 3. The compressive strength of the untreated FA geopolymer increased by 78.0%, from 19.9 MPa (0 wt.% CH) to 35.8 MPa (2 wt.% CH), which aligned with the bulk density result (Fig. 2). Incorporating 2 wt.% CH into FA geopolymers significantly improved compressive strength due to the presence of more OH⁻ ions, which encouraged the dissolution of FA, and led to the formation of more active species beneficial for polycondensation. The results were consistent with the study of Kim et al. [23], who concluded that the addition of 2 wt.% of CH was advantageous to the compressive strength of the metakaolin geopolymers.

Additionally, the compressive strength of FA geopolymers declined to 28.0 MPa with the increase of CH content up to 4 wt.%. The strength degradation was accounted to the delayed degree of reaction. According to Ilcan et al. [24], the inclusion of CH beyond 4 wt.% is not considerable. This is because the excess CH disrupted the reaction, suppressing the FA dissolution and limiting the availability of Si⁴⁺ and Al⁵⁺. Consequently, the reduced reactivity led to a non-homogeneous structure, ultimately deteriorating the mechanical strength.

The compressive strength of CH-incorporated FA geopolymers increased at 200°C, regardless of the CH contents. The increase in compressive strength (19.0%-35.9%) was attributed to the continued reaction of unreacted particles during the heating process. Besides, the addition of CH improved the mechanical performance by producing C-S-H in conjunction with N-A-S-H, resulting in a stable binary network capable of resisting high temperatures [22]. The compressive strength gradually reduced at 400-1000°C. The strength decrement at 400-600°C was due to the dehydration process, where progressive heating resulted in water evaporation within the FA geopolymers, inducing structural shrinkage and deterioration, such as cracks and pores.

The FA geopolymers began to melt and undergo phase transformation at 800°C, resulting in a weakened microstructure and

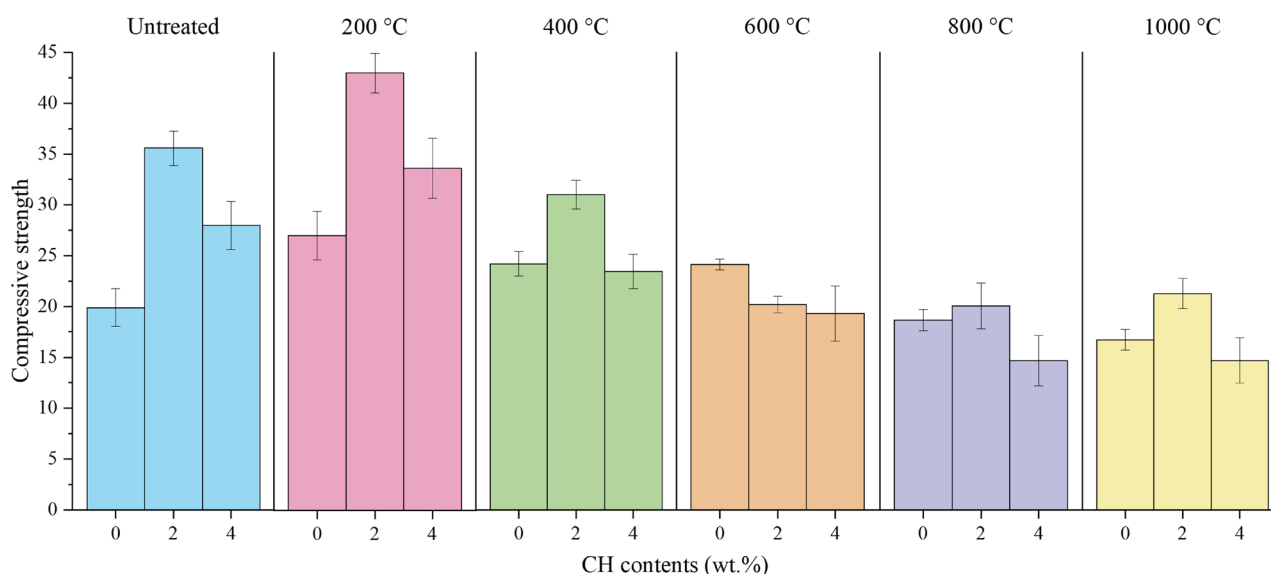


Fig. 3. Compressive strength of untreated and heat-treated FA geopolymers with varying CH contents

a subsequent decrement in compressive strength [25]. At 1000°C, the non-uniform transformation of the amorphous phase into the crystalline phase possibly caused disruption of the geopolymer network. This phenomenon facilitated stress concentration at the interface between the original amorphous phase and newly formed crystalline phase. As the stress intensified, cracks were initiated and propagated along the interface, leading to a collapsed microstructure [26], as shown in Fig. 4. Consequently, the compactness of the CH-incorporated FA geopolymers was compromised, and their compressive strength diminished.



Fig. 4. Mechanism of strength reduction during non-uniform phase transformation

In the present study, FA geopolymers incorporating 2 wt.% CH demonstrated optimal mechanical performance under heat exposure, particularly at 200°C. This characteristic is highly beneficial for industrial flooring application. In practical scenarios, the ability of building materials to withstand heat remains critically dependent on their mechanical strength. According to ASTM C1157 [27], the optimal geopolymers in this study achieved a compressive strength of 43.0 MPa, exceeding the minimum requirement of 28.0 MPa. Moreover, they attained peak compressive strength around 200°C (Fig. 3) and exhibited no spalling or physical damage (Fig. 1). Therefore, these ge-

opolymers are well-suited for heat-load environments. However, for applications involving exposure beyond 200°C, additional reinforcement or additives may be necessary to maintain the structural integrity and thermal stability.

Fig. 5 displays the SEM micrograph of the 200°C-treated FA geopolymer with varying CH contents at $\times 1000$ magnifications. The FA geopolymers without CH incorporation showed a microstructure with spherical particles, identified as unreacted FA (yellow-circled region) and pores. When CH was added (2 wt.%), the microstructure appeared more homogeneous with a minor amount of unreacted FA particles. This implied that the geopolymer effectively geopolymerized and densified when exposed to 200°C. The incorporation of CH triggered the chemical reaction between FA and alkaline solution, leading to the formation of micropores. In the meantime, the reaction products also filled the pores, resulting in a denser and stronger matrix (Fig. 2 and Fig. 3).

The red-circled regions suggested the plate-like structure recognized as C-S-H, which formed by the reaction of Ca (from CH) and the reactive Si, Al, and Na (from FA and alkali activators). A similar observation was reported by Pawluczuk et al. [28], where the plate-like C-S-H was found to improve the mechanical properties of the geopolymers. Additionally, the C-S-H interacted with Al^{5+} and Na^{+} [29], which are released during the continued geopolymerization process under heat exposure, contributing to the formation of hybrid network known as C,N-A-S-H that beneficial the mechanical properties [30,31]. Yet, C,N-A-S-H cannot be conclusively proven in this study and should be further investigated through X-ray Diffraction (XRD) in future research.

The microstructure of FA geopolymer with 4 wt.% CH (Fig. 5c) was smoother and the CH particles were evenly distributed (blue-circled region). The excessive CH particles functioned as obstacles that interlocked the geopolymer gel structure, resulting in a low compressive strength of FA geopolymer. The inert particles acted as stress concentrations or weak points, promoting crack development and propagation in geopolymer matrix.

Fig. 6 demonstrates the SEM micrograph of FA geopolymers with 4 wt.% CH at 200, 800, and 1000°C. A loosen microstructure was observed in FA geopolymer when subjected to 800°C. This was caused by the melting and phase transformation of the geopolymer networks at higher temperatures, as aforementioned. Despite the color changes, as previously mentioned,

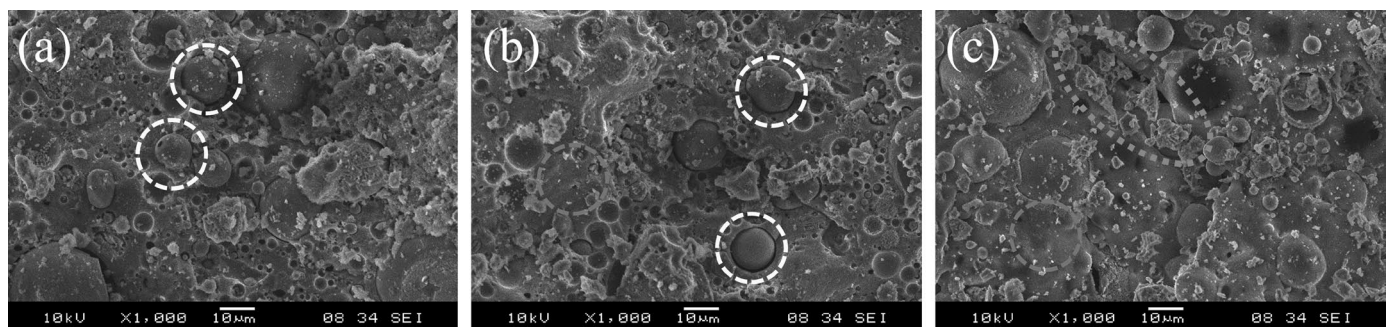


Fig. 5. SEM micrograph of FA geopolymers with (a) 0 wt.%, (b) 2 wt.%, and (c) 4. wt.% at 200°C

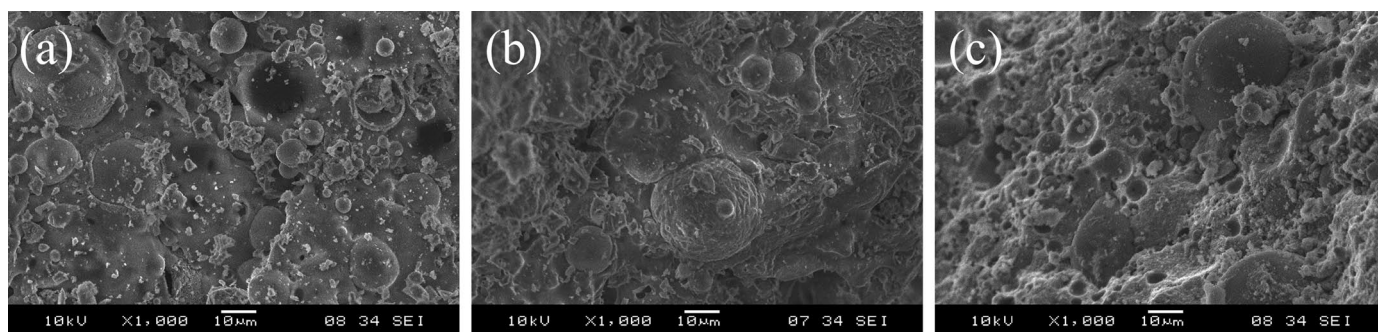


Fig. 6. SEM micrograph of FA geopolymers with 4 wt.% CH at (a) 200°C, (b) 800°C, and (c) 1000°C

the geopolymer does not melt completely, showing that the CH addition is still favorable for high-temperature stability. However, the microstructure of the geopolymer began to disintegrate around 1000°C where the amorphous gel started to break down (green-circled region) attributed to further crystallization, as aforementioned. The phase transformation results in structural deformation, reducing the compressive strength (Fig. 3).

The FTIR spectra of the heat-treated FA geopolymer are shown in Fig. 7, while TABLE 3 summarizes the main absorption peaks. The main band of the FA geopolymers was located around 970.0 cm^{-1} , which designated as the asymmetric vibration of Si-O-T bonding (T is Si or Al) [32]. The intensity of the band reflected the formation of the geopolymer framework. When the FA geopolymers incorporated to 2 wt.% CH, the intensity increased, indicating a large number of Al^{3+} was reacted with SiO_4 tetrahedral species. When treated at 800 and 1000°C, the in-

tensity decreased due to the destruction of geopolymer network.

The FA geopolymers showed a comparable absorption band to each other's. The absorption peak at approximately 3700.1-2300.2 cm^{-1} corresponded to O-H and H-O-H stretching vibration [33] due to the presence of minor moisture within the FA geopolymers. However, the intensity of the peak at 800 and 1000°C decreased, implying the diminish of moisture at elevated temperatures. The band of stretching vibration O-C-O was observed at $\sim 2170.1 \text{ cm}^{-1}$ and $\sim 2020.0 \text{ cm}^{-1}$ [34] due to the atmospheric carbonation of geopolymers. The band located at roughly 1650.4 cm^{-1} corresponded to the chemically bound water molecules (bending vibration O-H) [35]. In summary, the FTIR spectra indicated that the incorporation of CH did not lead to the presence of a new absorption peak, proving that CH was inert to the geopolymer formation. Nonetheless, heat treatment only altered the intensity of the existing peaks.

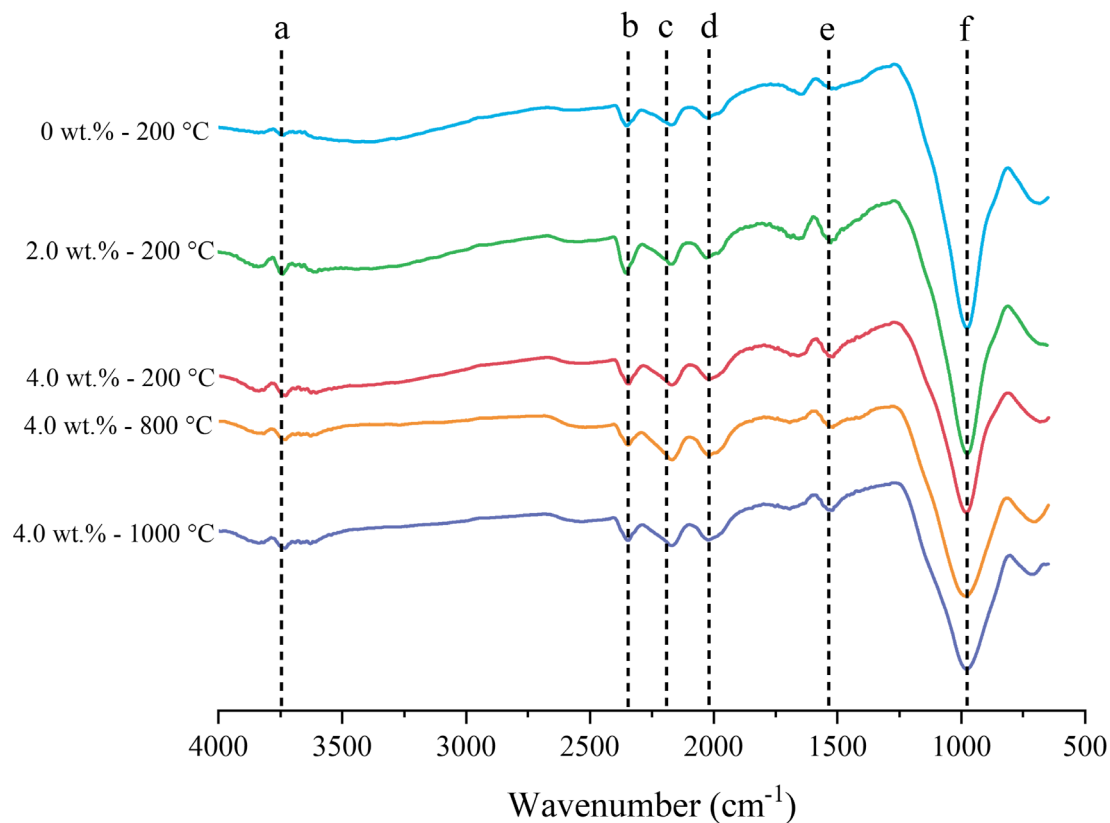


Fig. 7. The IR spectra of the heat-treated FA geopolymer with varying CH contents

TABLE 3
Absorption band of heat-treated FA geopolymers

Symbol	Wavenumber (cm ⁻¹)	Absorption band
a	3700.1-3740.6	O-H stretching vibration
b	2300.2-2352.3	Physical bound H-O-H
c	2170.1-2175.6	O-C-O stretching vibration
d	2020.0-2025.7	O-C-O stretching vibration
e	1650.4-1690.7	O-H bending vibration
f	970.0-980.2	Si-O-Si or Al asymmetrical vibration

4. Conclusion

This study investigated FA geopolymers with 0, 2, and 4 wt.% CH, evaluating their mechanical and morphological properties under heat exposure. The key findings are:

- The bulk density of FA geopolymers peaked at 1.8 g/cm³ with 2 wt.% CH but decreased to 1.7 g/cm³ at 4 wt.% CH due to excessive CH disrupting the reaction and causing rapid precipitation.
- FA geopolymers with 2 wt.% CH obtained the highest compressive strength (35.8 MPa), which was attributed to the coexistence of N-A-S-H and C-S-H, promoting their structural integrity.
- CH-incorporated FA geopolymers exhibited 12.8%-18.0% gains in bulk density when exposed to 200°C, but beyond this temperature, the bulk density gradually decreased.
- The compressive strength of CH-incorporated FA geopolymers increased to 43.0 MPa at 200°C due to the further geopolymerization but declined to 16.8 MPa at 1000°C due to moisture loss, structural cracking, and phase transformation.
- Morphological analysis revealed that the CH-incorporated FA geopolymers underwent structural deformation, including melting and phase transformation, disrupting the microstructure at 800-1000°C.

Considering all of these factors, 2 wt.% CH incorporation and 200°C heat exposure were optimal for enhancing the mechanical and morphological performances of FA geopolymers. This study provided a guideline into developing sustainable and thermally resistant construction binders, such as industrial flooring and thermal insulation structural walls.

REFERENCES

- [1] M. Wang, S. Luo, B.T. Pham, T.-C. Ling, J. Zhejiang Univ. Sci. A **24**, 886-897 (2023). DOI: <https://doi.org/10.1631/jzus.A2200571>
- [2] R. Mohamed, R. Abd Razak, M.M. Al Bakri Abdullah, L.A. Sofri, I.H. Aziz, N.F. Shahedan, Arch. Metall. Mater. **67**, (2022). DOI: <https://doi.org/10.24425/amm.2022.137791>
- [3] D.D. Burduhos-Nergis, P. Vizureanu, D.C. Achitei, A.V. Sandu, D.P. Burduhos-Nergis, M.M.A.B. Abdullah, Arch. Metall. Mater. **68**, (2023). DOI: <https://doi.org/10.24425/amm.2023.142444>
- [4] Y.H.M. Amran, R. Alyousef, H. Alabduljabbar, M. El-Zeadani, J. Clean. Prod. **251**, 119679 (2020). DOI: <https://doi.org/10.1016/j.jclepro.2019.119679>
- [5] X. Sun, J. Liu, Y. Zhao, J. Zhao, Z. Li, Y. Sun, J. Qiu, P. Zheng, J. Build. Eng. **60**, 105200 (2022). DOI: <https://doi.org/10.1016/j.jobte.2022.105200>
- [6] M. Mathapati, K. Amate, C. Durga Prasad, M.L. Jayavardhana, T. Hemanth Raju, Mater. Today Proc. **50**, 1535-1540 (2022). DOI: <https://doi.org/10.1016/j.matpr.2021.09.106>
- [7] M.M.A.B. Abdullah, I.H.A. Aziz, W.W.A. Zailani, S.Z.A. Rahim, H.C. Yong, A.V. Sandu, L.S. Peng, Arch. Metall. Mater. **67**, (2022). DOI: <https://doi.org/10.24425/amm.2022.141052>
- [8] A.A. Hoyos-Montilla, J.I. Tobón, F. Puertas, Cem. Concr. Compos. **137**, 104925 (2023). DOI: <https://doi.org/10.1016/j.cemconcomp.2022.104925>
- [9] S. Janga, A.N. Raut, M. Adamu, Y.E. Ibrahim, Powd. Techno. **444**, 120047 (2024). DOI: <https://doi.org/10.1016/j.powtec.2024.120047>
- [10] H. Yong-Jie, H. Cheng-Yong, L. Yun-Ming, M.M.A.B. Abdullah, L. Yeng-Seng, L. Wei-Hao, P. Pakawanit, K. Ern-Hun, O. Shee-Ween, J. Build. Eng. **87**, 109096 (2024). DOI: <https://doi.org/10.1016/j.jobte.2024.109096>
- [11] B. Ma, Y. Luo, L. Zhou et al., Constr. Build. Mater. **329**, 127224 (2022). DOI: <https://doi.org/10.1016/j.conbuildmat.2022.127224>
- [12] A.G. Borçato, M. Thiesen, R.A. Medeiros-Junior, J. Build. Eng. **88**, 109259 (2024). DOI: <https://doi.org/10.1016/j.jobte.2024.109259>
- [13] M. Samadi, L.S. Wong, G. Murali, N.H.A.S. Lim, I.S. Ayeni, J. Build. Eng. **91**, 109692 (2024). DOI: <https://doi.org/10.1016/j.jobte.2024.109692>
- [14] M. Verma, R.K. Meena, I. Singh, N. Gupta, K.K. Saxena, M.M. Reddy, K.H. Salem, U. Salmaan, Adv. Mech. Eng. **15**, 16878132231196402 (2023). DOI: <https://doi.org/10.1177/16878132231196402>
- [15] H.Y. Zhang, G.H. Qiu, V. Kodur, Z.S. Yuan, Cem. Concr. Compos. **106**, 103483 (2020). DOI: <https://doi.org/10.1016/j.cemconcomp.2019.103483>
- [16] K.M.L. Alventosa, B. Wild, C.E. White, Cem. Concr. Res. **154**, 106742 (2022). DOI: <https://doi.org/10.1016/j.cemconres.2022.106742>
- [17] Y. Hu, Z. Shao, J. Wang, J. Zang, L. Tang, F. Ma, B. Qian, B. Ma, L. Wang, J. Build. Eng. **45**, 103521 (2022). DOI: <https://doi.org/10.1016/j.jobte.2021.103521>
- [18] P. Zhang, X. Han, S. Hu, J. Wang, T. Wang, Compos. Part B Eng. **244**, 110171 (2022). DOI: <https://doi.org/10.1016/j.compositesb.2022.110171>
- [19] X. Jiang, Y. Zhang, R. Xiao, P. Polaczyk, M. Zhang, W. Hu, Y. Bai, B. Huang, J. Clean. Prod. **270**, 122500 (2020). DOI: <https://doi.org/10.1016/j.jclepro.2020.122500>
- [20] Y. Lv, J. Qiao, W. Han, B. Pan, X. Jin, H. Peng, Mater. **16**, 2305 (2023). DOI: <https://doi.org/10.3390/ma16062305>
- [21] Saloni, Parveen, Y. Yan Lim, T.M. Pham, Constr. Build. Mater. **300**, 124321 (2021). DOI: <https://doi.org/10.1016/j.conbuildmat.2021.124321>

- [22] A. Mehta, R. Siddique, T. Ozbakkaloglu, F. Uddin Ahmed Shaikh, R. Belarbi, *Constr. Build. Mater.* **257**, 119548 (2020).
DOI: <https://doi.org/10.1016/j.conbuildmat.2020.119548>
- [23] B. Kim, S. Lee, C.-M. Chon, S. Cho, *Mater.* **15**, 194 (2022).
DOI: <https://doi.org/10.3390/ma15010194>
- [24] H. Ilcan, O. Sahin, A. Kul, G. Yildirim, M. Sahmaran, *Constr. Build. Mater.* **328**, 127114 (2022).
DOI: <https://doi.org/10.1016/j.conbuildmat.2022.127114>
- [25] A.M. Tahwia, O. El-Far, M. Amin, *Innov. Infrastruc. Solut.* **7**, 8 (2021). DOI: <https://doi.org/10.1007/s41062-021-00609-7>
- [26] J.C. Kuri, S. Majhi, P.K. Sarker, A. Mukherjee, *J. Build. Eng.* **43**, 103099 (2021).
DOI: <https://doi.org/10.1016/j.jobe.2021.103099>
- [27] ASTM C1157, ASTM (Am. Soc. Test Mater.) Spec. Tech. Publ., (2019).
- [28] E. Pawluczuk, K. Kalinowska-Wichrowska, J.R. Jiménez, J.M. Fernández-Rodríguez, D. Suescum-Morales, *J. Build. Eng.* **44**, 103317 (2021).
DOI: <https://doi.org/10.1016/j.jobe.2021.103317>
- [29] B. Walkley, R. San Nicolas, M.-A. Sani, G.J. Rees, J.V. Hanna, J.S.J. van Deventer, J.L. Provis, *Cem. Concr. Res.* **89**, 120-135 (2016). DOI: <https://doi.org/10.1016/j.cemconres.2016.08.010>
- [30] Y. Luo, H.J.H. Brouwers, Q. Yu, *Cem. Concr. Res.* **170**, 107198 (2023).
DOI: <https://doi.org/10.1016/j.cemconres.2023.107198>
- [31] N. Yong-Sing, L. Yun-Ming, H. Cheng-Yong, M.M.A.B. Abdullah, C. Rojviriyi, M.S. Khalid, O. Shee-Ween, O. Wan-En, H. Yong-Jie, *J. Build. Eng.* **69**, 106331 (2023).
DOI: <https://doi.org/10.1016/j.jobe.2023.106331>
- [32] H. Yong-Jie, H. Cheng-Yong, L. Yun-Ming et al., *Constr. Build. Mater.* **427**, 136264 (2024).
DOI: <https://doi.org/10.1016/j.conbuildmat.2024.136264>
- [33] C. Bai, J. Shao, X. Li, Z. Zhang, Y. Qiao, J. Hao, H. Li, T. Zheng, P. Colombo, *Mater. Lett.* **308**, 131158 (2022).
DOI: <https://doi.org/10.1016/j.matlet.2021.131158>
- [34] N. Hui-Teng, H. Cheng-Yong, L. Yun-Ming et al., *J. Non-Crystal. Solids* **585**, 121527 (2022).
DOI: <https://doi.org/10.1016/j.jnoncrysol.2022.121527>
- [35] G. Gu, T. Ma, F. Chen, F. Xu, J. Zhang, *Cem. Concr. Compos.* **129**, 104503 (2022).
DOI: <https://doi.org/10.1016/j.cemconcomp.2022.104503>